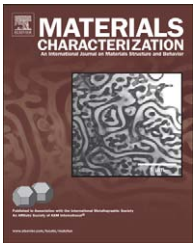

Prediction and characterization of growth temperatures in Al–Zn–Mg alloys

M.A. Suarez[a,*], A.G. Lara[b], F.M. Sánchez-Arévalo[b], O. Alvarez[b], J. Colin[c], J.A. Juarez-Islas[b]

[a]Facultad de Química, Universidad Nacional Autónoma de México (UNAM), Circuito Exterior S/N, Cd. Universitaria, C.P. 04510. México, D.F.
[b]Instituto de Investigaciones en Materiales, UNAM, Circuito Exterior S/N, Cd. Universitaria, C.P. 04510, México, D.F.
[c]Facultad de Ciencias Químicas e Ingeniería-UNAM, Av Universidad 1001, Col Chamipla, Cuernavaca, Morelos, México

ARTICLE DATA

Article history:
Received 3 March 2008
Received in revised form 16 April 2008
Accepted 5 November 2008

Keywords:
Aluminum alloys
Competitive growth
Unidirectional solidification
Predictions
Microstructural characterization

ABSTRACT

Growth temperatures of α-Al, intermetallic τ and eutectic α+τ phases in Al-12 wt.% Zn 6 wt.% Mg alloy has been determined as a function of growth velocity in the range of 3×10^{-5} to 1×10^{-3} m/s at a temperature gradient of 2500 K/m, using a directional solidification technique. The experimental results are found to be in good agreement with predictions of growth temperatures of competing constituents for multicomponent systems.

1. Introduction

The resulting microstructures in binary or multiphase alloys, in the velocity range at the solid/liquid interface from the critical growth velocity for constitutional supercooling (V_{cs}) to absolute stability (V_{ab}), consist mainly of a cellular or dendritic structure with eutectic in the intercellular or interdendritic spaces. Depending of element solute content in the alloy and the limit conditions imposed on the system during the solidification, other phases can be formed at the moving solid/liquid interface. It is very important to model the growth of primary phases, eutectic, or intermetallic compounds, for the purpose of describing microstructural evolution [1].

The growth temperature (T_G), of competing constituents such as primary phases and eutectics, plays a critical role in determining the constitution and morphology of the resulting microstructures of solidification under specific conditions; few direct measurements have been made regarding the dependence of T_G, on the solidification variables, (growth velocity, V, and the composition of the alloy (C_0)), particularly for dendritic structures [2–7].

The purpose of the present work is to measure experimentally the growth temperatures of α-Al, intermetallic τ and eutectic α+τ phases as a function of growth velocity (V), in the range of 3×10^{-5} to 1×10^{-3} m/s and to compare the results with predictions of a multicomponent systems model. An Al-12 wt.% Zn-6 wt.% Mg alloy has been chosen for this study because there are numerous experimental results in the literature and well defined physical properties.

2. Dendritic Growth

In order to carry out the predictions of the resulting solidification microstructures as a function of the solidification front, it is considered that during dendritic growth the dendrite tip undercooling ΔT (T_L–T_G), will depend on the

* *Corresponding author*. Tel.: +52 56 22 54 89; fax: +52 56 16 13 61.
E-mail address: msuarez@iim.unam.mx (M.A. Suarez).

1044-5803/$ – see front matter © 2008 Elsevier Inc. All rights reserved.
doi:10.1016/j.matchar.2008.11.002

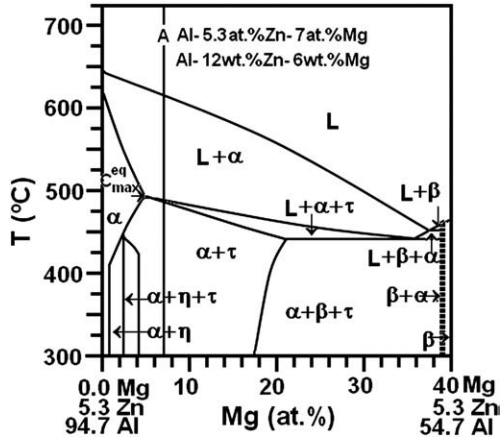

Fig. 1 – Vertical section at constant 5.3 at.% (12 wt.%) Zn of the ternary Al–Zn–Mg phase diagram [11]. The vertical line shows the master alloy composition designated as A.

temperature gradient (G_L), growth velocity, (V) and alloy composition (C_0) according with [8]:

$$\Delta T = \frac{G_L D_L}{V} + B_1 (V)^n \tag{1}$$

where D_L is the liquidus solute diffusion coefficient, B_1 is a constant for dendrite growth, n is the velocity exponent that depends of growth morphology and is typically close to 0.5. In the case when $D_L G_L / V << B_1 (V)^{1/2}$, Eq. (1) becomes:

$$\Delta T = B_1 V^{1/2} \tag{2}$$

It is also assumed that Eq. (2) can apply for both equiaxed dendritic and columnar growth. In addition, it can be used to determine the growth temperature of competing constituents under particular conditions [1]. Typically, the growth temperature, $T_{G\alpha}$ for dendrites has been represented as [8,9]:

$$T_L - T_{G,\alpha-Al} = B_1 V^{1/2} \tag{3}$$

where

$$B_1 = \left[\frac{2\pi^2 \Gamma m_L (k-1) C_0}{D_L}\right]^{1/2} \tag{3a}$$

and for multicomponent systems the constant B_1 it is expressed as:

$$B_1 = \left[2\pi^2 \left\{\sum_{i=1}^{n} \frac{\Gamma_i m_i (k_i - 1) C_{Li}^{*2} \rho_i}{D_{Li} \sum_{j=1}^{n} C_{Lj}^{*} \rho_j}\right\}^{1/2}\right] \tag{3b}$$

where T_L and $T_{G,\alpha-Al}$, are the liquidus and growth temperatures respectively, Γ is the Gibbs–Thompson parameter, m_L the liquidus slope, k the partition coefficient, ρ the density, D_L is the liquidus solute diffusion coefficient and C_{Lj}^{*} is the liquid composition at the dendrite tip.

The growth temperature, $T_{G\tau}$., for the intermetallic growth has been represented as [1,9]:

$$T_L - T_{G,\tau} = B_2 V^{1/3} \tag{4}$$

where

$$B_2 = [m_L (k-1) C_0]^{2/3} \left[\frac{\Gamma}{Dk}\right]^{1/3} \tag{4a}$$

and for multicomponent systems, the constant B_2, it is expressed as:

$$B_2 = \left[\sum_{i=1}^{n} \frac{\Gamma_i m_i^2 C_{Li}^{*3} \rho_i}{k_i D_{Li} \sum_{j=1}^{n} C_{Lj}^{*} \rho_j}\right]^{1/3} \tag{4b}$$

The growth temperature T_{GEu}, for the eutectic growth is predicted and found experimentally [9,10] to conform with:

$$T_{Eu} - T_{G,Eu} = A_1 V^{1/2} \tag{5}$$

where A_1 is a constant for eutectic growth.

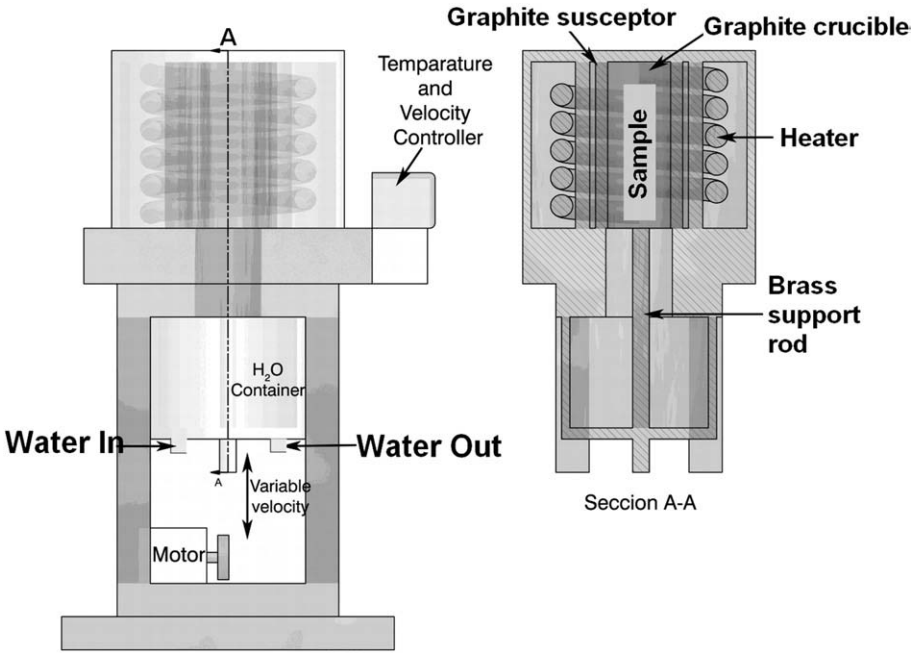

Fig. 2 – Schematic diagram of the experimental apparatus for unidirectional solidification.

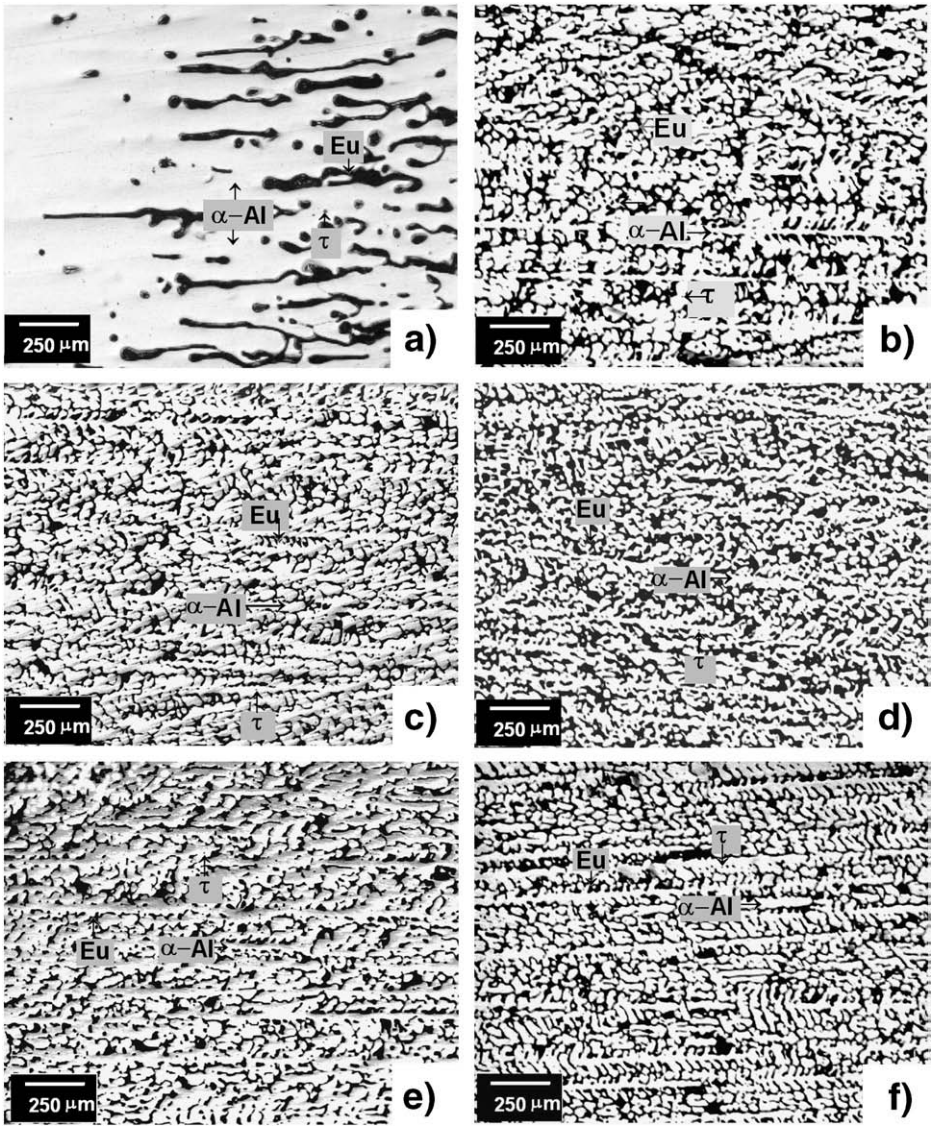

Fig. 3 – Microstructural morphology of Al-12wt.%Zn-6wt.%Mg alloy unidirectionally solidified at velocities of: a) 4×10^{-6} m/s; b) 3×10^{-5} m/s; c) 7×10^{-5} m/s; d) 1.3×10^{-4} m/s; e) 1.7×10^{-4} m/s and f) 1×10^{-3} m/s.

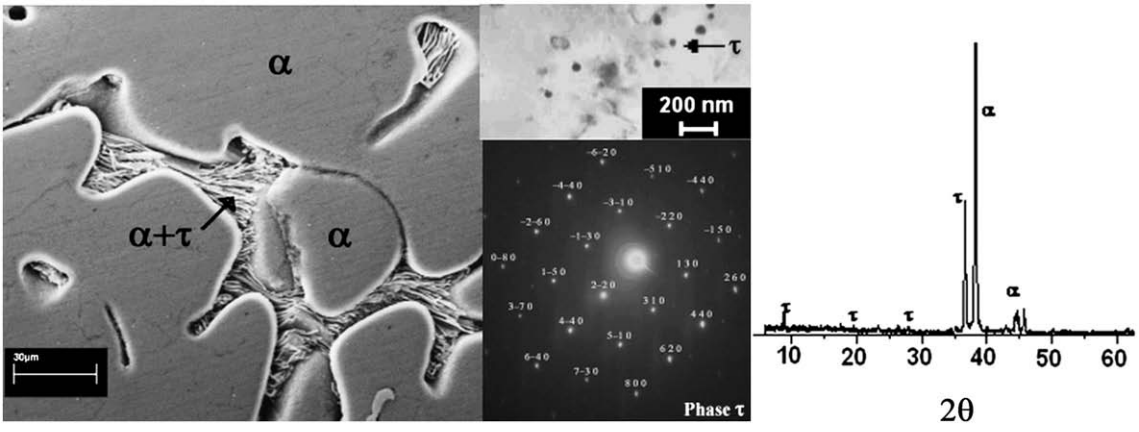

Fig. 4 – SEM micrograph of Al- 12 wt.%Zn-6 wt.%Mg alloy indicated microstructure that consists mainly by α-Al phase with (α+τ) eutectic in interdendritic regions. Precipitates in α-Al matrix were identified as the intermetallic τ (right hand side) using electron diffraction pattern and X-ray diffractometry.

3. Experimental

Alloy of Al-12wt.%Zn-6wt.%Mg designated as A (see Fig. 1), was prepared from high purity (99.99%) aluminum, zinc (99.9%) and magnesium (99.9%) elements by vacuum induction melting under a constant flux of argon and cast into a copper mould of cavity dimension 25 mm thick, 50 mm wide and 120 mm high. The alloy composition is between the maximum concentration of solute at equilibrium C^{eq}_{max} and the $\alpha+\tau$ field, as indicated in the phase diagram of Fig. 1 [11]. Rods of 3×10^{-3} m in diameter and 0.12 m of length were fabricated directly from the ingots, which were poured into prepared cylindrical graphite crucibles (0.15 m in length, 3×10^{-3} m ID and 6.3×10^{-3} m OD) and unidirectionally solidified using a Bridgman-modified equipment shown in Fig. 2.

During the unidirectional solidification experiments, the temperature of the alloy was kept 100 °C above the liquidus temperatures for about 30 min and then, the alloy was unidirectionally solidified at growth velocities in the range of 3×10^{-5} to 1×10^{-3} m/s with an imposed temperature gradient of 2500 °C/m. In order to measure the growth temperature of the solid/liquid interface throughout the solidification, two cromel/alumel type K thermocouples (3×10^{-4} m in diameter) were placed into holes drilled in the sample, separated 1×10^{-2} m from tip to tip. Thermocouple output was recorded during the solidification and recorded as a plot of temperature versus time using an acquisition system.

The unidirectionally solidified specimen was removed from the graphite crucible, a longitudinal section was ground, polished and etched with Kellers reagent and the microstructure and microanalyses were carried out with both light optical and scanning electron microscopes (LOC and SEM).

4. Results and Discussion

4.1. Microstructural Characterization

As can be seen in Fig. 1, when cooling of liquid alloy A reached the $L+\alpha$ region, the first phase to nucleate is the α-Al, and as the temperature decreases until the $L+\alpha+\tau$ region is reached, phases such as the intermetallic τ and eutectic are formed. The microstructures observed in the alloy under study consisted mainly of columnar dendrites of α-Al, eutectic $\alpha+\tau$ ($Al_2Mg_3Zn_3$) in interdendritic regions and τ ($Al_2Mg_3Zn_3$) intermetallic in α-Al matrix as is shown in Fig. 3, where a set of

Table 1 – Input data for the model predictions

From the equilibrium phase diagram	Physical properties of Al–Zn–Mg system	
Región $L+\alpha$	$D_{L,Zn}=8.8\times10^{-8}$ m²/s	[12]
$m_L=-3.93$ K/wt.%	$D_{L,Mg}=9.45\times10^{-9}$ m²/s	[12]
$k=0.141$	$\Gamma_{Zn}=1.52\times10^{-7}$ Km	[13]
$T_{L,A}=893$K		
Región $L+\alpha+\tau$	$\Gamma_{Mg}=9.87\times10^{-7}$Km	[13]
$m_L=-1.45$ K/wt.%	$G_L=25$–30 °C/cm	present work
$k=0.687$	$A_1=51.2$ Ks$^{1/2}$/m$^{1/2}$	[14]
$T_{L,A}=758$K		
$T_{L,EU}=715.6$K		

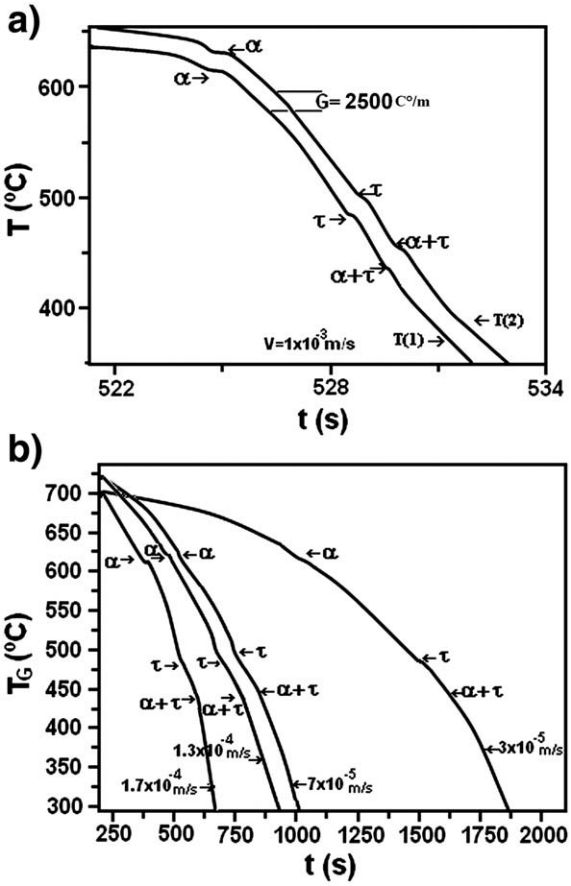

Fig. 5 – Cooling curves of the Al-12 wt.%Zn-6 wt.%Mg alloy at growth velocities of: a) 1×10^{-3} m/s; b) 3×10^{-5}–1.7×10^{-4} m/s solidified at a thermal gradient G=2500 °C/m.

representative unidirectional solidified microstructures are presented for the Al-12 wt.% Zn-6 wt.% Mg alloy solidified at velocities from 3×10^{-5} to 1×10^{-3} m/s. Identification of τ intermetallic was performed by X-ray diffractography and its electron diffraction pattern is shown in Fig. 4.

4.2. Competitive Growth and Thermal Analysis

In order to predict the resulting microstructure during solidification of Al–Zn–Mg alloys as a function of solidification growth velocity, the growth temperature was first plotted for α-Al from the $L+\alpha$ region, assuming that the only competing constituents will be the α-Al and the $\alpha+\tau$-eutectic phases. For this purpose Eqs. (3b) and (5) were employed. To predict the eutectic growth, Eq. (5) was employed, feeding a value of 51.2 Ks$^{1/2}$/m$^{1/2}$ for the constant A, derived during the experiments. To predict dendrite, intermetallic and eutectic growth for the $L+\alpha+\tau$ region, Eqs. (3b), (4b) and (5) were employed. To solve the above equations, the equilibrium temperatures for α-Al and eutectic were taken from the equilibrium phase diagram as shown in Table 1. In the same table, the values of k, m_L, D_L and Γ, for the $L+\alpha$ and $L+\alpha+\tau$ regions are shown.

Fig. 5(a,b) show representative cooling curves obtained during unidirectional solidification of Al-12 wt.% Zn-6 wt.% Mg alloy in the growth velocities range from 3×10^{-5} to1×10^{-3} m/s. The thermal arrest indicated in this figure results from the

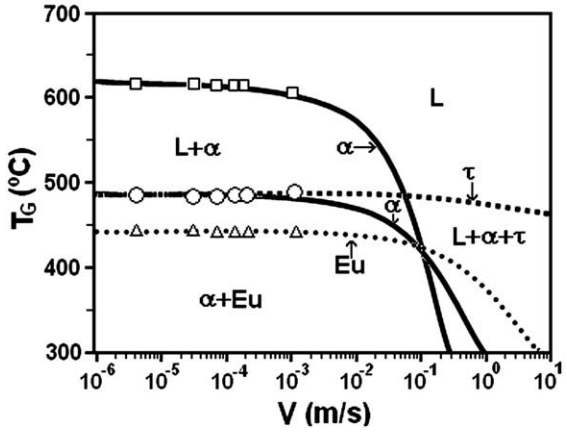

Fig. 6 – Predictions of T_G vs. V, for Al-12 wt.%Zn-6 wt.%Mg alloy. The symbols □$T_{G,\alpha}$, ○$T_{G,\tau}$, and Δ $T_{G,Eu}$, represent the experimental growth temperatures of α-Al, τ intermetallic and (α+τ) eutectic phases in the range velocity from 3×10^{-5} to 1×10^{-3} m/s.

passage of the solidification front and thus indicates a growth temperature. The temperature of initial departure was indicative of α-Al tip temperature, followed by growth temperatures of τ intermetallic and (α+τ) eutectic. Fig. 6 shows the predicted microstructure during the solidification of Al-12wt.%Zn-6wt.%Mg alloy as a plot of growth temperature versus growth velocity and the growth temperatures of phases obtained experimentally. As is observed, during solidification of the alloy in the $L+\alpha$ region, the only phase that growth is the α-Al, as the cooling proceed and the solidification path reached the $L+\alpha+\tau$ region, both the α-Al and the intermetallic τ will grow simultaneously up to a growth velocity of 1×10^{-3} m/s. As the growth velocity increased, the intermetallic compound will be the only one to grow. Finally, the last dotted curve shows the growth temperatures for eutectic $\alpha+\tau$, in which it is predicted that this phase will be the dominant phase at very high growth velocities.

5. Conclusions

Thermal analysis together with microstructural characterization permits the derivation of growth temperatures for α-Al, intermetallic τ ($Al_2Mg_3Zn_3$) and eutectic $\alpha+\tau$ in the ternary Al–Zn–Mg system as a function of composition and growth velocity.

The experimental results are found to be in good agreement with predictions of growth temperatures of competing constituents for multicomponent systems at solidification front velocities up to 1×10^{-3} m/s.

Results showed that $T_{G,\alpha}$, $T_{G,\tau}$, and $T_{G,\ EU}$, decreases with increase in growth velocity.

Acknowledgments

The authors acknowledge the financial support from Consejo Nacional de Ciencia y Tecnología (CONACYT). We also thank to O.Novelo, L. Baños, E. Fregoso and C. Flores for the technical support.

REFERENCES

[1] Jones H. On array model theoretical calculations versus measurements for the growth undercooling of aluminide dendrites in Bridgman solidified aluminium alloys. Scr Mater 2001;45:95–101.
[2] Kurz W, Fisher DJ. Dendrite growth at the limit of stability: tip radius and spacing. Acta Metall 1981;29:11–20.
[3] Liang D, Jones H. The dependence of growth temperature on growth velocity for primary Al_3Fe in steady solidification of hypereutectic Al–Fe alloys. Scr Metall Mater 1991;25:2855–9.
[4] Liang D, Gilgien P, Jones H. Effect of silicon alloying additions on growth temperature and primary spacing of Al_3Fe in Al-8 wt.% Fe alloy. Scr Metall Mater 1995;32:1513–8.
[5] Kurz W, Giovanola B, Trivedy R. Theory of microstructural development during rapid solidification. Acta Met 1986;34:823–30.
[6] Liang D, Jones H. Predictions of the Hunt-Lu array model compared with measurements for the growth undercooling of Al_3Fe dendrites in Al–Fe alloys. Scr Metall Mater 1997;37:911–3.
[7] Liang D, Jones H. The dependence of growth temperature on alloy concentration for primary Al_3Fe in steady state solidification of Al–Fe alloys. Scr Metall Mater 1993;28:7–10.
[8] Tassa M, Hunt JD. The measurements of Al–Cu dendrite tip and eutectic interface temperatures and their use for predicting the extent of the eutectic range. J Cryst Growth 1976;34:38–48.
[9] Alvarez O, Gonzales C, Aramburo G, Herrera R, Juarez-Islas JA. Characterization and prediction of microstructure in Al–Zn–Mg alloys. Mater Sci Eng 2005;402A:320–4.
[10] Juarez-Hernandez A, Jones H. Growth temperature measurements and solidification microstructure selection of primary Al_3Ni and eutectic in the α-Al–Al_3Ni system. Scr Metall Mater 1998;38:729–34.
[11] Petrov DA, Petzow G, Effemberg, editors. Ternary Alloys, vol. 3. Weinheim, Germany: VCH; 1986. p. 57.
[12] Peterson NL, Rothman SJ. Phys Rev B: Solid State 1970;1:3264.
[13] Deryagin BV, Friedland RM. Zh Tekh Fiz 1984;18:1443.
[14] Liang H, Chang YA. Mat Mater Trans 1997;28A:1725.